

Search for the Blazhko effect in field RR Lyrae stars using LINEAR and ZTF light curves

2 EMA DONEV¹ AND ŽELJKO IVEZIĆ²

3 ¹*XV. Gymnasium (MIOC), Jordanovac 8, 10000, Zagreb, Croatia*

4 ²*Department of Astronomy and the DiRAC Institute, University of Washington, 3910 15th Avenue NE, Seattle, WA 98195, USA*

5 ABSTRACT

6 We analyzed the incidence and properties of RR Lyrae stars that show evidence for amplitude and
7 phase modulation (the so-called Blazhko Effect) in a sample of \sim 3,000 stars with LINEAR and ZTF
8 light curve data collected during the periods of 2002–2008 and 2018–2023, respectively. A preliminary
9 subsample of about \sim 500 stars was algorithmically pre-selected using various data quality and light
10 curve statistics, and then 228 stars were confirmed visually as displaying the Blazhko effect. This
11 sample increases the number of field RR Lyrae stars displaying the Blazhko effect by more than 50%
12 and places a lower limit of $(11.4 \pm 0.8)\%$ for their incidence rate. We find that ab type RR Lyrae
13 that show the Blazhko effect have about 5% (0.030 day) shorter periods than starting sample, a 7.1σ
14 statistically significant difference. We find no significant differences in their light curve amplitudes and
15 apparent magnitude (essentially, signal-to-noise ratio) distributions. No period or other differences are
16 found for c type RR Lyrae. We find convincing examples of stars where the Blazhko effect can appear
17 and disappear on time scales of several years. With time-resolved photometry expected from LSST, a
18 similar analysis will be performed for even larger samples of fields RR Lyrae stars in the southern sky
19 and we anticipate a higher fraction of discovered Blazhko stars due to better sampling and superior
20 photometric quality.

21 **Keywords:** Variable stars — RR Lyrae variable stars — Blazhko effect

22 1. INTRODUCTION

23 RR Lyrae stars are pulsating variable stars with per-
24 iodds in the range of 3–30 hours and large amplitudes that
25 increase towards blue optical bands (e.g., in the SDSS *g*
26 band from 0.2 mag to 1.5 mag; [Sesar et al. 2010](#)). For
27 comprehensive reviews of RR Lyrae stars, we refer the
28 reader to [Smith \(1995\)](#) and [Catelan \(2009\)](#).

29 RR Lyrae stars often exhibit amplitude and phase
30 modulation, or the so-called Blazhko effect¹ (hereafter,
31 “Blazhko stars”). For examples of well-sampled observed
32 light curves showing the Blazhko effect, see, e.g., Ke-
33 pler data shown in Figures 1 and 2 from [Benkő et al.](#)
34 ([2010](#)). The Blazhko effect has been known for a long
35 time ([Blažko 1907](#)), but its detailed observational prop-
36 erties and theoretical explanation of its causes remain
37 elusive ([Kolenberg 2008](#); [Kovács 2009](#); [Szabó 2014](#)). Var-
38 ious proposed models for the Blazhko effect, and prin-

39 cipal reasons why they fail to explain observations, are
40 summarized in [Kovacs \(2016\)](#).

41 A part of the reason for the incomplete observational
42 description of the Blazhko effect is difficulties in discov-
43 ering a large number of Blazhko stars due to tempo-
44 ral baselines that are too short and insufficient number
45 of observations per object ([Kovacs 2016](#); [Hernitschek &](#)
46 [Stassun 2022](#)). With the advent of modern sky sur-
47 veys, several studies reported large increases in the num-
48 ber of known Blazhko stars, starting with a sample of
49 about 700 Blazhko stars discovered by the MACHO sur-
50 vey towards the LMC ([Alcock et al. 2003](#)) and about
51 500 Blazhko stars discovered by the OGLE-II survey
52 towards the Galactic bulge ([Mizerski 2003](#)). Most re-
53 cently, about 4,000 Blazhko stars were discovered in the
54 LMC and SMC ([Soszyński et al. 2009, 2010](#)), and an
55 additional \sim 3,500 stars were discovered in the Galactic
56 bulge ([Soszyński et al. 2011](#); [Prudil & Skarka 2017](#)), both
57 by the OGLE-III survey. Nevertheless, discovering the
58 Blazhko effect in field RR Lyrae stars that are spread
59 over the entire sky remains a much harder problem: only
60 about 400 Blazhko stars in total ([Skarka 2013](#)) from all
61 the studies of field RR Lyrae stars have been reported
62 so far (see also Table 1 in [Kovacs 2016](#)).

Corresponding author: Željko Ivezić
ivezic@uw.edu

¹ The Blazhko effect was probably discovered by Lidiya Petrovna Tseraskaya and first reported by Sergey Blazhko though exact discovery details remain unclear.

63 Here, we report the results of a search for the Blazhko
 64 effect in a sample of $\sim 3,000$ field RR Lyrae stars with
 65 LINEAR and ZTF light curve data. A preliminary sub-
 66 sample of about ~ 500 stars was selected using various
 67 light curve statistics, and then 228 stars were confirmed
 68 visually as displaying the Blazhko effect. This new sam-
 69 ple doubles the number of field RR Lyrae stars that
 70 exhibit the Blazhko effect. In §2 and §3 we describe our
 71 datasets and analysis methodology, and in §4 we present
 72 our analysis results. Our main results are summarized
 73 and discussed in §5.

74

75 2. DATA DESCRIPTION AND PERIOD 76 ESTIMATION

77 Analysis of field RR Lyrae stars requires a sensitive
 78 time-domain photometric survey over a large sky area.
 79 For our starting sample, we used $\sim 3,000$ field RR Lyrae
 80 stars with light curves obtained by the LINEAR aster-
 81 oid survey. In order to study long-term changes in light
 82 curves, we also utilized light curves obtained by the ZTF
 83 survey which monitored the sky ~ 15 years after LIN-
 84 EAR. The combination of LINEAR and ZTF provided
 85 a unique opportunity to systematically search for the
 86 Blazhko effect in a large number of field RR Lyrae stars
 87 over a large time span of two decades.

88 We first describe each dataset in more detail, and then
 89 introduce our analysis methods. All our analysis code,
 90 written in Python, is available on GitHub².

91

2.1. LINEAR Dataset

92 The properties of the LINEAR asteroid survey and
 93 its photometric re-calibration based on SDSS data are
 94 discussed in Sesar et al. (2011). Briefly, the LINEAR
 95 survey covered about 10,000 deg² of the northern sky
 96 in white light (no filters were used, see Fig. 1 in Sesar
 97 et al. 2011), with photometric errors ranging from ~ 0.03
 98 mag at an equivalent SDSS magnitude of $r = 15$ to 0.20
 99 mag at $r \sim 18$. Light curves used in this work include,
 100 on average, 270 data points collected between December
 101 2002 and September 2008.

102 A sample of 7,010 periodic variable stars with $r < 17$
 103 discovered in LINEAR data were robustly classified by
 104 Palaversa et al. (2013), including about $\sim 3,000$ field RR
 105 Lyrae stars of both ab and c type, detected to distances
 106 of about 30 kpc (Sesar et al. 2013). The sample used
 107 in this work contains 2196 ab-type and 745 c-type RR
 108 Lyrae, selected using classification labels and the *gi* color
 109 index from Palaversa et al. (2013). The LINEAR light
 110 curves, augmented with IDs, equatorial coordinates, and
 111 other data, were accessed using the astroML Python
 112 module³ (VanderPlas et al. 2012).

113

2.2. ZTF Dataset

114 The Zwicky Transient Factory (ZTF) is an opti-
 115 cal time-domain survey that uses the Palomar 48-inch
 116 Schmidt telescope and a camera with 47 deg² field of
 117 view (Bellm et al. 2019). The dataset analyzed here
 118 was obtained with SDSS-like *g*, *r*, and *i* band filters.
 119 Light curves for objects in common with the LINEAR
 120 RR Lyrae sample typically have smaller random photo-
 121 metric errors than LINEAR light curves because ZTF
 122 data are deeper (compared to LINEAR, ZTF data have
 123 about 2-3 magnitudes fainter 5 σ depth). ZTF data used
 124 in this work were collected between February 2018 and
 125 December 2023, on average about 15 years after obtain-
 126 ing LINEAR data. The median number of observations
 127 per star for ZTF light curves is ~ 500 .

128 The ZTF dataset for this project was created by se-
 129 lecting ZTF IDs with matching equatorial coordinates to
 130 a corresponding LINEAR ID of an RR Lyrae star. This
 131 process used the *ztfquery* function, which searched the
 132 coordinates in the ZTF database within 3 arcsec from
 133 the LINEAR position. The resulting sample consisted of
 134 2857 RR Lyrae stars with both LINEAR and ZTF data.
 135 The fractions of RRab and RRc type RR Lyrae in this
 136 sample, 71% RRab and 29% RRc type, are consistent
 137 with results from other surveys (e.g., Sesar et al. 2010;
 138 Clementini et al. 2023).

139

2.3. Period Estimation

140 The first step of our analysis is estimating best-fit peri-
 141 ods, separately for LINEAR and ZTF datasets. We used
 142 the Lomb-Scargle method (Vanderplas 2015) as imple-
 143 mented in *astropy* (Astropy Collaboration et al. 2018).
 144 The period estimation used 3 Fourier components and
 145 a two-step process: an initial best-fit frequency was de-
 146 termined using the *autopower* frequency grid option and
 147 then the power spectrum was recomputed around the
 148 initial frequency using an order of magnitude smaller
 149 frequency step. In case of ZTF, we estimated period
 150 separately for each available passband and adopted their
 151 median value. Once the best-fit period was determined,
 152 a best-fit model for the phased light curve was computed
 153 using 6 Fourier components. Fig 1 shows an example of
 154 a star with LINEAR and ZTF light curves, phased light
 155 curves, and their best-fit models.

156 We found excellent agreement between the best-fit
 157 periods estimated separately from LINEAR and ZTF
 158 light curves. The median of their ratio is unity within
 159 2×10^{-6} and the robust standard deviation of their ratio
 160 is 2×10^{-5} . With a median sample period of 0.56 days,
 161 the implied scatter of period difference is about 1.0 sec.

162 Given on average about 15 years between LINEAR
 163 and ZTF data sets, and a typical period of 0.56 days,
 164 this time difference corresponds to about 10,000 oscilla-
 165 tions. With a fractional period uncertainty of 2×10^{-5} ,
 166 LINEAR data can predict the phase of ZTF light curve
 167 with an uncertainty of 0.2. RR Lyrae light curves may
 168 experience phase changes of this magnitude (see e.g.,

² https://github.com/emadonev/var_stars

³ For an example of light curves, see https://www.astroml.org/book_figures/chapter10/fig_LINEAR_LS.html

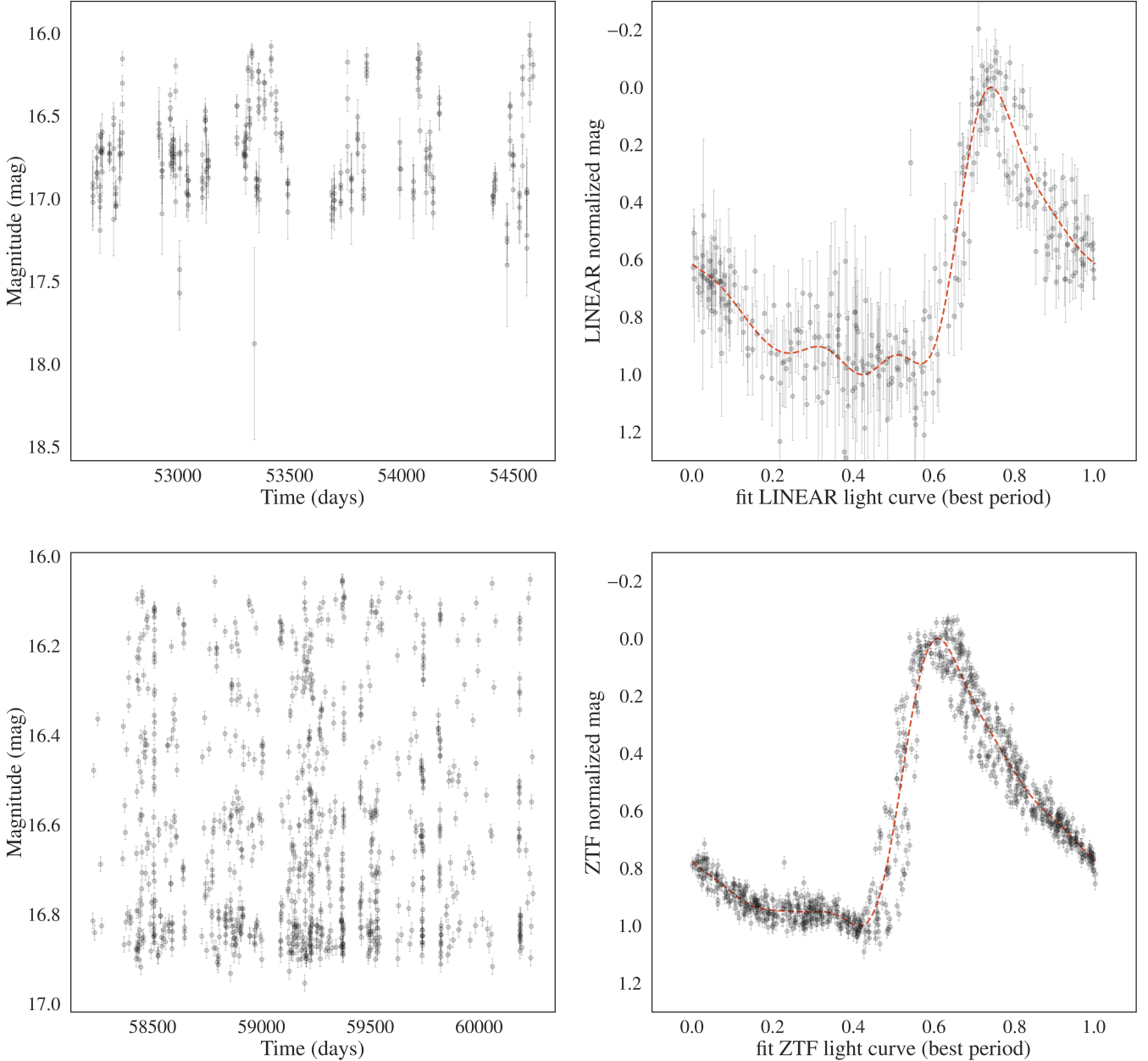


Figure 1. An example of a Blazhko star (LINEARid = 136668) with LINEAR (top row; period = 0.532923 day) and ZTF (bottom row; period = 0.532929 day) light curves (left panels, data points with “error bars”), phased light curves normalized to the 0–1 range (right panels, data points with “error bars”), with their best-fit models shown by dashed lines. The best-fit period is determined for each dataset separately using 3 Fourier terms. The models shown in the right panels are evaluated with 6 Fourier terms.

¹⁶⁹ Szeidl et al. 2011; Dagne et al. 2017); therefore, each
¹⁷⁰ data set must be analyzed separately. On the other
¹⁷¹ hand, amplitude modulation can be detected on time
¹⁷² scales as long as 15 years, as discussed in the following
¹⁷³ section.

¹⁷⁴ We did not try to identify double-mode (RRd) stars
¹⁷⁵ because their expected sample fraction is below 1%
¹⁷⁶ (Clementini et al. 2023).

¹⁷⁷ 3. ANALYSIS METHODOLOGY: SEARCHING FOR ¹⁷⁸ THE BLAZHKO EFFECT

¹⁷⁹ Given the two sets of light curves from LINEAR and
¹⁸⁰ ZTF, we searched for amplitude and phase modulation,
¹⁸¹ either during the 5–6 years of data taking by each sur-
¹⁸² vey, or during the average span of 15 years between
¹⁸³ the two surveys. Starting with a sample of 2857 RR
¹⁸⁴ Lyrae stars, we pre-selected a smaller sample that was
¹⁸⁵ inspected visually (see below for details). We also re-
¹⁸⁶ quired at least 150 LINEAR data points and 150 ZTF

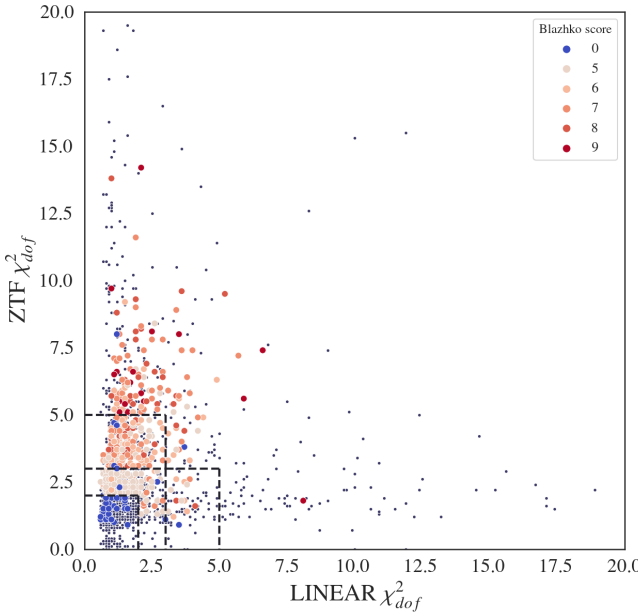


Figure 2. A selection diagram constructed with the two sets of robust χ^2_{dof} values, for LINEAR and ZTF data sets, where the dark blue dots represent all RR Lyrae stars and the circles represent candidate Blazhko stars (color-coded according to the legend, with B_score representing the number of points scored from the selection algorithm). The horizontal and vertical dashed lines help visualize selection boundaries for Blazhko candidates (see text).

187 data points (for the selected band from which we cal-
188 culated the period) in analyzed light curves. We used
189 two pre-selection methods that are sensitive to differ-
190 ent types of light curve modulation: direct light curve
191 analysis and periodogram analysis, as follows.

192 3.1. Direct Light Curve Analysis

193 Given statistically correct period, amplitude and light
194 curve shape estimates, as well as data being consistent
195 with reported (presumably Gaussian) uncertainty esti-
196 mates, the χ^2 per degree of freedom gives a quantitative
197 assessment of the "goodness of fit",

$$198 \quad \chi^2_{dof} = \frac{1}{N_{dof}} \sum \frac{(d_i - m_i)^2}{\sigma_i^2}. \quad (1)$$

199 Here, d_i are measured light curve data values at times
200 t_i , and with associated uncertainties σ_i , m_i are best-
201 fit models at times t_i , and N_{dof} is the number of de-
202 grees of freedom, essentially the number of data points.
203 In the absence of any light curve modulation, the ex-
204 pected value of χ^2_{dof} is unity, with a standard devia-
205 tion of $\sqrt{2/N_{dof}}$. If $\chi^2_{dof} - 1$ is many times larger than
206 $\sqrt{2/N_{dof}}$, it is unlikely that data d_i were generated by
207 the assumed (unchanging) model m_i . Of course, χ^2_{dof}
208 can also be large due to underestimated measurement

209 uncertainties σ_i , or to occasional non-Gaussian measure-
210 ment error (the so-called outliers).

211 Therefore, to search for signatures of the Blazhko ef-
212 fect, manifested through statistically unlikely large val-
213 ues of χ^2_{dof} , we computed χ^2_{dof} separately for LINEAR
214 and ZTF data (see Fig. 2). Using the two sets of χ^2_{dof}
215 values, we algorithmically pre-selected a sample of can-
216 didate Blazhko stars for further visual analysis of their
217 light curves. The visual analysis is needed to confirm
218 the expected Blazhko behavior in observed light curves,
219 as well as to identify cases of data problems, such as
220 photometric outliers.

221 We used a simple scoring algorithm, optimized
222 through trial and error, that utilized the two values of
223 χ^2_{dof} , augmented by period and amplitude differences, as
224 follows. A star could score a maximum of 9 points, and
225 a minimum of 5 points was required for further visual
226 analysis. The χ^2_{dof} selection boundaries are illustrated
227 in Fig. 2. If either value of χ^2_{dof} exceeded 5, or both ex-
228 ceeded 3, a star was awarded 5 points and immediately
229 selected for further analysis. If these χ^2_{dof} criteria were
230 not met, a star could still be selected by meeting less
231 stringent χ^2_{dof} selection if it also had large period or am-
232 plitude difference between LINEAR and ZTF datasets.
233 Stars with at least one value of χ^2_{dof} above 2 would re-
234 ceive 3 points and those with at least one χ^2_{dof} above
235 3 would receive 4 points. A period difference exceeding
236 2×10^{-4} day would be awarded 1 point and two points for
237 exceeding 5×10^{-4} day. Analogous limits for amplitude
238 difference were 0.05 mag and 0.15 mag, respectively.

239 The candidate Blazhko sample pre-selected using this
240 method includes 531 stars. For most selected stars, the
241 χ^2_{dof} values were larger for the ZTF data because the
242 ZTF photometric uncertainties are smaller than for the
243 LINEAR data set. Fig. 3 summarizes the selection cri-
244 teria and the resulting numbers of selected stars for each
245 criterion and their combinations.

246 3.2. Periodogram Analysis

247 When light curve modulation is due to double-mode
248 oscillation with two similar oscillation frequencies (peri-
249 ods), it is possible to recognize its signature in the peri-
250 odogram computed as part of the Lomb-Scargle analy-
251 sis. Depending on various details, such as data sampling
252 and the exact values of periods, amplitudes, this method
253 may be more efficient than direct light curve analysis
254 (Skarka et al. 2020). We also employed this method to
255 select additional candidates, as follows.

256 A sum of two *sine* functions with same amplitudes
257 and with frequencies f_1 and f_2 can be rewritten using
258 trigonometric equalities as

$$259 \quad y(t) = 2 \cos(2\pi \frac{f_1 - f_2}{2} t) \sin(2\pi \frac{f_1 + f_2}{2} t). \quad (2)$$

260 We can define

$$261 \quad f_o = \frac{f_1 + f_2}{2}, \quad (3)$$

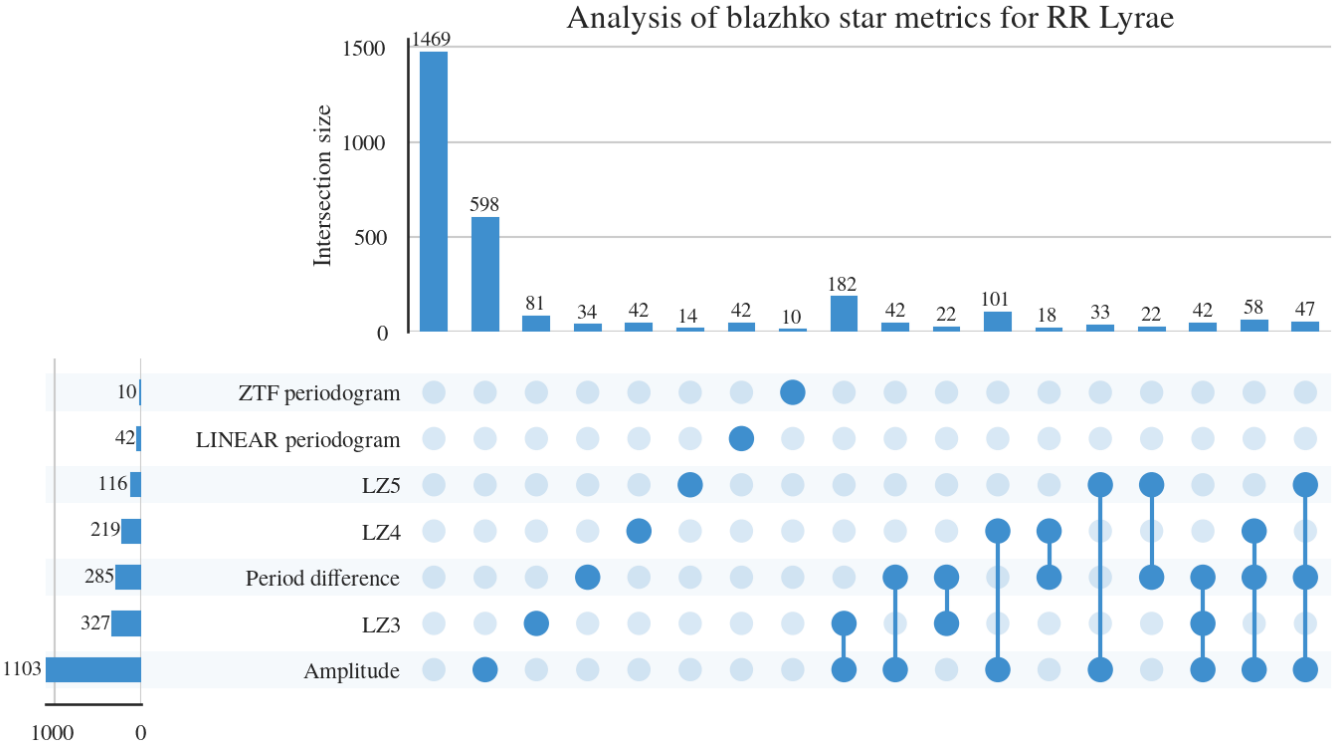


Figure 3. The figure shows selection criteria and the resulting numbers of pre-selected Blazhko star candidates for each criterion and their combinations (x in LZx corresponds to the number of scored points in the χ^2_{dof} vs. χ^2_{dof} diagram (see Fig. 2)). The dots represent each case a star can occupy, where every solid dot is a specific criterion that is satisfied. Connections between solid dots represent stars which satisfy multiple criteria. Each dot combination has its own count, represented by the horizontal countplot. The vertical countplot shows the total number of stars that satisfy one criteria (union of all cases). For example, a total of 116 stars passed the LZ5 criterion, with 14 of them satisfying only χ^2 criterion, 33 also had a significant amplitude change, 22 had a significant period difference, and 47 had both a significant period and amplitude difference along with the satisfied χ^2 criterion. The sum of all specific cases is 116.

and

$$\Delta f = \left| \frac{f_1 - f_2}{2} \right|, \quad (4)$$

with $\Delta f \ll f_o$ when f_1 and f_2 are similar. The fact that Δf is much smaller than f_o means that the period of the *cos* term is much larger than the period of the basic oscillation (f_o). In other words, the *cos* term acts as a slow amplitude modulation of the basic oscillation. When the amplitudes of two *sine* functions are not equal, the results are more complicated but the basic conclusion about amplitude modulation remains. When the power spectrum of $y(t)$ is constructed, it will show 3 peaks: the main peak at f_o and two more peaks at frequencies $f_o \pm \Delta f$. We used this fact to construct an algorithm for automated searching for the evidence of amplitude modulation. Fig 4 compares the theoretical periodogram produced by interference beats with our algorithm's periodogram, signifying that local Blazhko peaks are present in real data.

After the strongest peak in the Lomb-Scargle periodogram is found at frequency f_o , we search for two equally distant local peaks at frequencies f_- and f_+ ,

with $f_- < f_o < f_+$. The sideband peaks can be highly asymmetric (Alcock et al. 2003) and observed periodograms can sometimes be much more complex (Szczygieł & Fabrycky 2007). We fold the periodogram through the main peak at f_o , multiply the two branches and then search for the strongest peaks in the resulting folded periodogram that is statistically more significant than the background noise. The multiplication of the two branches allows for efficient detection of moderately asymmetric peaks. However, this method is not sensitive to the subset of modulated stars where only one sidepeak is detectable (Netzel et al. 2018; Molnár et al. 2023). The background noise is computed as the scatter of the folded periodogram estimated from the interquartile range. We require a “signal-to-noise” ratio of at least 5, as well as the peak strength of at least 0.05 for ZTF, while 0.10 for LINEAR data. If such a peak is found, and it doesn't correspond to yearly alias, we select the star as a candidate Blazhko star and compute its Blazhko period as

$$P_{BL} = |f_{-,+} - f_o|^{-1},$$

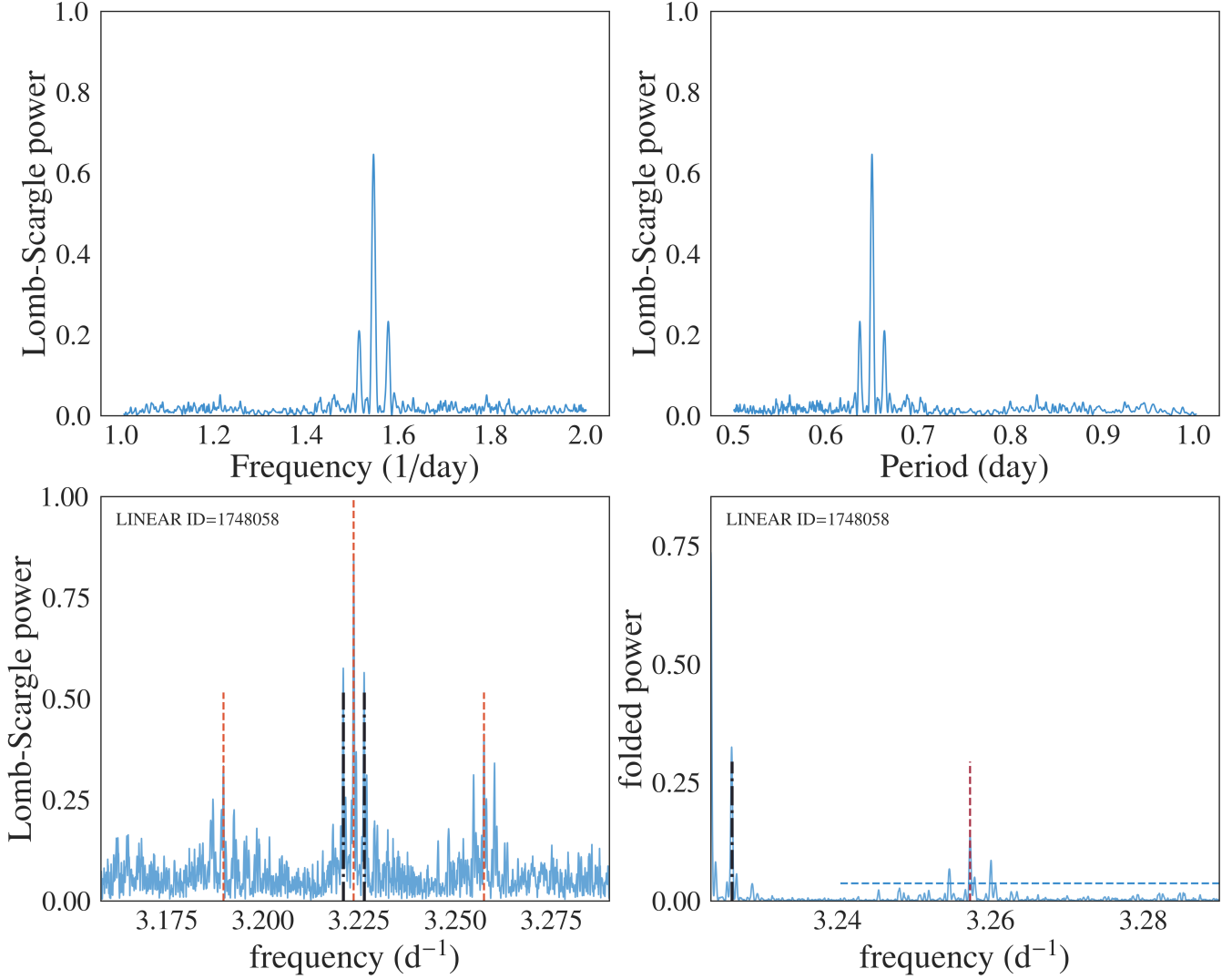


Figure 4. The top two panels show a simulated periodogram for a sum of two *sine* functions with similar frequencies f_1 and f_2 – the central peak corresponds to their mean (see eqs. 3 and 4). The bottom left panel shows a periodogram for an observed LINEAR light curve for $ID = 1748058$, and the bottom right panel shows its folded version (around the main frequency $f_o = 3.223 \text{ d}^{-1}$). In the bottom left panel, the three vertical dashed lines show the three frequencies identified by the algorithm described in text, and the two dot-dashed lines mark yearly aliases around the main frequency f_o , at frequencies $f_o \pm 0.0274 \text{ d}^{-1}$. The two vertical lines in the bottom right panel have the same meaning, and the horizontal dashed line shows the noise level multiplied by 5.

where $f_{-,+}$ means the Blazhko sideband frequency with a higher amplitude is chosen.

The observed Blazhko periods range from 3 to 3,000 days, and Blazhko amplitudes range from 0.01 mag to about 0.3 mag (Szczygieł & Fabrycky 2007). In this work, we selected a smaller Blazhko range due to the limitations of our data: 30–325 days. With this additional constraint, we selected 52 candidate Blazhko stars. Fig. 4 shows an example where two very prominent peaks were identified in the LINEAR periodogram.

3.2.1. Visual Confirmation

The sample pre-selected for visual analysis includes 531 RR Lyrae stars ($479 + 52$), or 18.1% of the starting LINEAR-ZTF sample. Visual analysis included the following standard steps (e.g., Jurcsik et al. 2009; Prudil & Skarka 2017):

1. The shape of the phased light curves and scatter of data points around the best-fit model were examined for signatures of anomalous behavior indicative of the Blazhko effect. Fig. 6 shows an example of such behavior where the ZTF data and fit show multiple coherent data point sequences offset from the best-fit mean model.

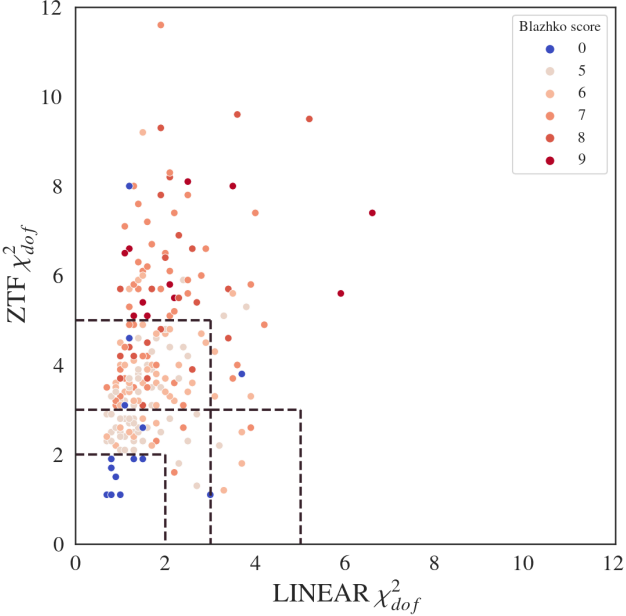


Figure 5. Analogous to figure 2, except that here only 228 visually verified Blazhko stars are shown.

2. Full light curves were inspected for their repeatability between observing seasons (Fig. 7). This step was sensitive to amplitude modulations with periods of the order a year or longer.
3. The phased light curves normalized to unit amplitude were inspected for their repeatability between observing seasons. This step was sensitive to phase modulations of a few percent or larger on time scales of the order a year or longer. Fig. 8 shows an example of a Blazhko star where season-to-season phase and amplitude modulations are seen in both the LINEAR data and (especially) the ZTF data. Another example is shown in Fig. 9 where only phase modulation is visible, without any discernible amplitude modulation⁴.

After visually analyzing the starting sample of 531 Blazhko candidates, we visually confirmed expected Blazhko behavior for 228 stars (214 out of 479 and 14 out of 52). LINEAR IDs and other characteristics for confirmed Blazhko stars are listed in Table 1 (Appendix A). Statistical properties of the selected sample of Blazhko stars are discussed in detail in the next section.

4. RESULTS

Starting with a sample of 2857 field RR Lyrae stars with both LINEAR and ZTF data, we constructed a

⁴ The physical reason for large phase modulations remains unclear: stellar companions may cause small variations through the light-time effect (Hajdu et al. 2021), but some RRc stars show phase variations well exceeding that (e.g., Derekas et al. 2004; Sóder et al. 2017; Le Borgne & Klotz 2019).

subsample of 1996 with light curves of sufficient quality and selected and verified 228 stars that exhibit convincing Blazhko effect. In this section we compare various statistical properties of selected Blazhko stars to those of the starting sample.

4.1. The Blazhko Incidence Rate

The implied incidence rate for the Blazhko effect is $11.4 \pm 0.8\%$. Due to selection effects and unknown completeness, this rate should be considered as a lower limit. When ab and c types are considered separately, the rate is slightly higher for the former than for the latter: $12.1 \pm 0.9\%$ vs. $9.2 \pm 1.3\%$. The difference of 2.9% has low statistical significance ($< 2\sigma$).

4.2. Period, Amplitude and Magnitude Distributions

Marginal distributions of period, amplitude and apparent magnitude for the starting sample and Blazhko stars are compared in Fig. 10. Encouragingly, their magnitude distributions are statistically indistinguishable which indicates that the completeness is not a strong function of the photometric signal-to-noise ratio. This result is probably due to the fact that the sample is defined by the depth of LINEAR survey, while ZTF survey is deeper than this limit and its photometric quality is approximately constant across the probed magnitude range.

The suspected differences in amplitude and period distributions are further explored in Fig. 11. It is already discernible by eye that the period distribution for Blazhko stars of ab type is shifted to smaller values than for the starting sample. We have found that the median period for ab type Blazhko stars is about 5% shorter than for the starting RR Lyrae sample. This difference is significant at the 7.1σ level. At the same time, the difference in median amplitudes for ab type stars corresponds to only 0.6σ deviation. No statistically significant differences are found in period and amplitude distributions for c type stars.

If modulation amplitudes are correlated with periods such that larger modulation amplitudes occur in shorter period RRab stars, and if our selection efficiency is lower for smaller modulation amplitudes, then the detected period shift for ab type Blazhko stars might be at least partially due to combination of these two effects. This possibility does not appear likely. First, as we discussed in preceeding section, our sample is defined by the depth of LINEAR survey, while ZTF survey is significantly deeper than this limit and its photometric quality is approximately constant across the probed magnitude range. Since it is sufficient for a star to display the Blazhko effect only in ZTF to be included in the sample, we do not expect strong selection effects (except for the LINEAR magnitude cutoff of course). Furthermore, Skarka et al. (2020) searched for period - modulation amplitude correlation using a large sample of stars with OGLE measurements and did not find any.

STAR 1140 from 2857

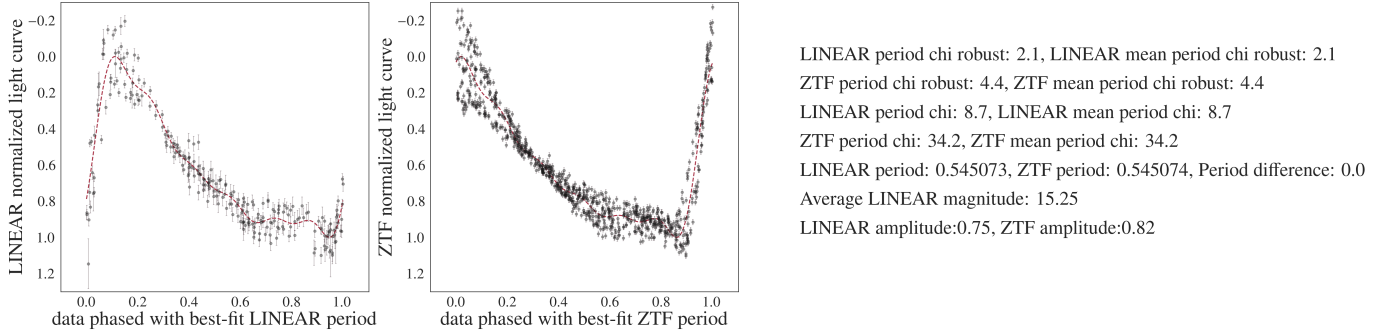


Figure 6. An illustration of visual analysis of phased light curves for the selected Blazhko candidates. The left panel shows LINEAR data and the right panel shows ZTF data (symbols with “error bars”) for star with LINEARid = 10030349. The dashed lines are best-fit models. The numbers listed on the right side were added to aid visual analysis. Note multiple coherent data point sequences offset from the best-fit mean model in the right panel.

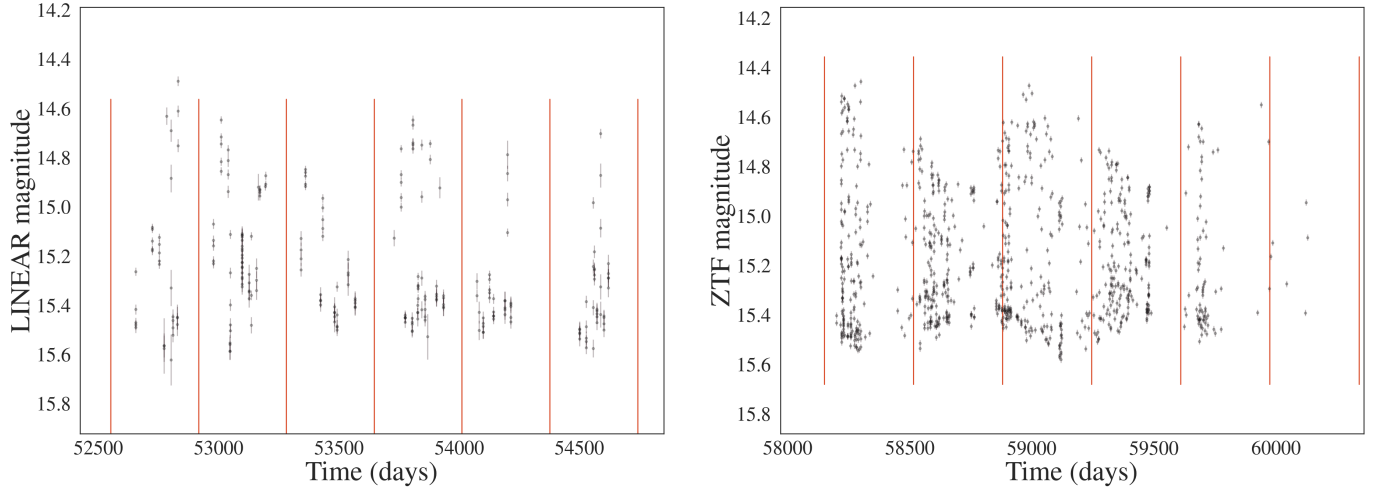


Figure 7. An illustration of visual analysis of full light curves for the selected Blazhko candidates with emphasis on their repeatability between observing seasons, marked with vertical lines (left: LINEAR data; right: ZTF data). Data shown are for star with LINEARid = 10030349. Note strong amplitude modulation between observing seasons.

4.3. Long-term behavior of Blazhko Stars

During visual analysis, we noticed that some Blazhko stars exhibit convincing Blazhko effect either in LINEAR or in ZTF data, but not in both surveys. Fig. 12 shows an example where amplitude modulation is clearly seen in LINEAR light curves, while not discernible in ZTF light curves. There are also examples of stars where Blazhko effect is evident in ZTF but not in LINEAR data (e.g., LINEARid = 19466437, 14155360). This finding strongly suggests that Blazhko effect can appear and disappear on time scales shorter than about a decade.

5. DISCUSSION AND CONCLUSIONS

We found excellent agreement between the best-fit periods for RR Lyrae stars estimated separately from LINEAR and ZTF light curves. Only one star in our sample (CT CrB, LINEARid=17919686), was previously re-

ported as a Blazhko star (Skarka 2013). The sample of 228 stars presented here increases the number of field RR Lyrae stars displaying the Blazhko effect by more than 50% and places a lower limit of $(11.4 \pm 0.8)\%$ for their incidence rate. The reported incidence rates for the Blazhko effect range from 5% (Szczygieł & Fabrycky 2007) to 60% (Szabó et al. 2014). Differences in reported incidence rates can occur due to varying data precision, the temporal baseline length, and differences in visual or algorithmic analysis. For a relatively small sample of 151 stars with Kepler data, a claim has been made that essentially every RR Lyrae star exhibits modulated light curve (Kovacs 2018). The difference in Blazhko incidence rates for the two most extensive samples, obtained by the OGLE-III survey for the Large Magellanic Cloud (LMC, 20% out of 17,693 stars; Soszyński et al. 2009) and the Galactic bulge (30% out of 11,756 stars; Soszyński et al. 2011) indicates a possible variation of

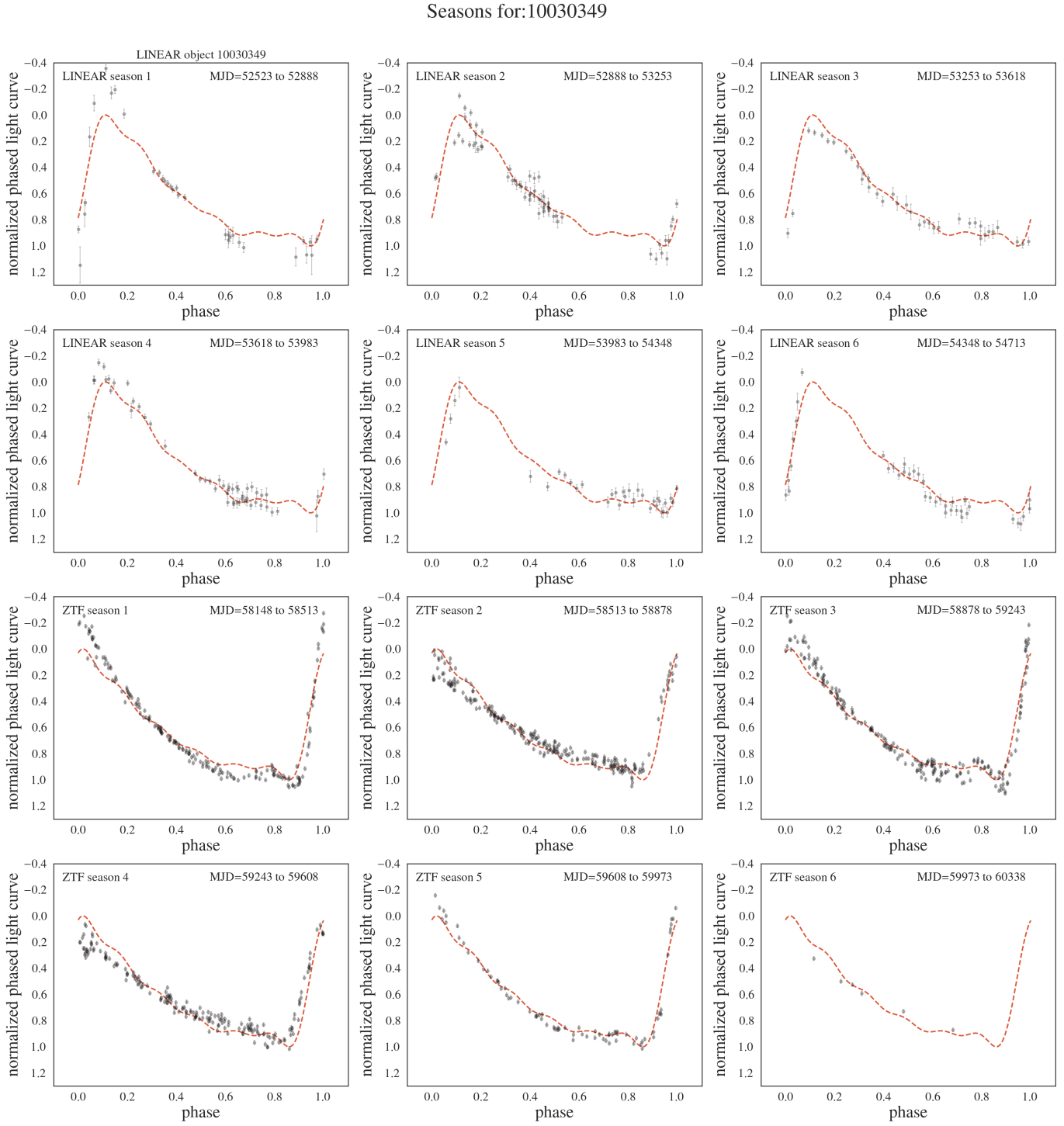


Figure 8. The phased light curves normalized to unit amplitude of the overall best-fit model are shown for single observing seasons and compared to the mean best-fit models (top six panels: LINEAR data; bottom six panels: ZTF data). Data shown are for star with LINEARid = 10030349 (period = 0.54073 day). Season-to-season phase and amplitude modulations are seen in both the LINEAR and the ZTF data.

the Blazhko incidence rate with underlying stellar population properties.

We find that ab type RR Lyrae which show the Blazhko effect have about 5% (0.030 day) shorter periods than starting sample. While not large, the statistical significance of this difference is 7.1σ . At a similar uncertainty level ($\sim 1\%$), we don't detect period difference for c type stars, and don't detect any difference in amplitude distributions. We also find that for some stars the Blazhko effect is discernible in only one dataset. This finding strongly suggests that Blazhko effect can appear and disappear on time scales shorter than about a decade, in agreement with literature (Jurcsik et al. 2009; Poretti et al. 2010; Benkő et al. 2014).

The LINEAR and ZTF datasets analyzed in this work were sufficiently large that we had to rely on algorithmic pruning of the initial sample. The sample size problem will be even larger for surveys such as the Legacy Survey of Space and Time (LSST; Ivezić et al. 2019). LSST will be an excellent survey for studying Blazhko effect (Hernitschek & Stassun 2022) because it will have both a long temporal baseline (10 years) and a large number of observations per object (nominally 825; LSST Science Requirements Document⁵). We anticipate a higher fraction of discovered Blazhko stars with LSST than reported here due to better sampling and superior photometric quality, since the incidence rate of the Blazhko effect increases with sensitivity to small-amplitude modulation, and thus with photometric data quality (Jurcsik et al. 2009).

The size and quality of LSST sample will motivate further developments of the selection algorithms. One obvious improvement will be inspection of neighboring objects to confirm photometric quality, as well as inspection of images to test implication of an isolated point source (e.g., blended object photometry can be affected by variable seeing beyond aperture correction valid for isolated point sources). Another improvement is forward modeling of the Blazhko modulation, rather than searching for χ^2 outliers (Benkő et al. 2011; Guggenberger et al. 2012). For example, Skarka et al. (2020)

classified Blazhko stars in 6 classes using the morphology of their amplitude modulation (the most dominant class includes 90% of the sample). They also found bimodal distribution of Blazhko periods, with two components centered on 48 d and 186 d. These results give hope that forward modeling of the Blazhko effect will improve the selection of such stars.

We thank Mathew Graham for providing *ztfquery* code example to us, and Robert Szabó for expert comments that improved presentation.

Ž.I. acknowledges funding by the Fulbright Foundation and thanks the Ruđer Bošković Institute (Zagreb, Croatia) for hospitality.

Based on observations obtained with the Samuel Oschin Telescope 48-inch and the 60-inch Telescope at the Palomar Observatory as part of the Zwicky Transient Facility project. ZTF is supported by the National Science Foundation under Grants No. AST-1440341 and AST-2034437 and a collaboration including current partners Caltech, IPAC, the Weizmann Institute of Science, the Oskar Klein Center at Stockholm University, the University of Maryland, Deutsches Elektronen-Synchrotron and Humboldt University, the TANGO Consortium of Taiwan, the University of Wisconsin at Milwaukee, Trinity College Dublin, Lawrence Livermore National Laboratories, IN2P3, University of Warwick, Ruhr University Bochum, Northwestern University and former partners the University of Washington, Los Alamos National Laboratories, and Lawrence Berkeley National Laboratories. Operations are conducted by COO, IPAC, and UW.

The LINEAR program is funded by the National Aeronautics and Space Administration at MIT Lincoln Laboratory under Air Force Contract FA8721-05-C-0002. Opinions, interpretations, conclusions and recommendations are those of the authors and are not necessarily endorsed by the United States Government.

Software: Astropy (Astropy Collaboration et al. 2018, 2022), Matplotlib (Hunter 2007), SciPy (Virtanen et al. 2020), astroML (VanderPlas et al. 2012)

523

APPENDIX

Table 1: The first 10 confirmed Blazhko stars with their LINEAR IDs in the first column and then, for both LINEAR and ZTF, their computed light curve periods (day), the number of data points per light curve, robust and ordinary χ^2 values, and light curve amplitudes, followed by amplitude difference between LINEAR and ZTF, the strength and period of Blazhko peaks in their periodograms, light curve type (1: ab, 2: c), detection significance flag for the periodograms (Z, L or “-” for no detection; the strength and period of Blazhko peaks are not reliable when “-”) and the selection score (see Sections 3.1 and 3.2 for details). The full table is available in online edition.

⁵ Available as ls.st/srd

Seasons for:16300450

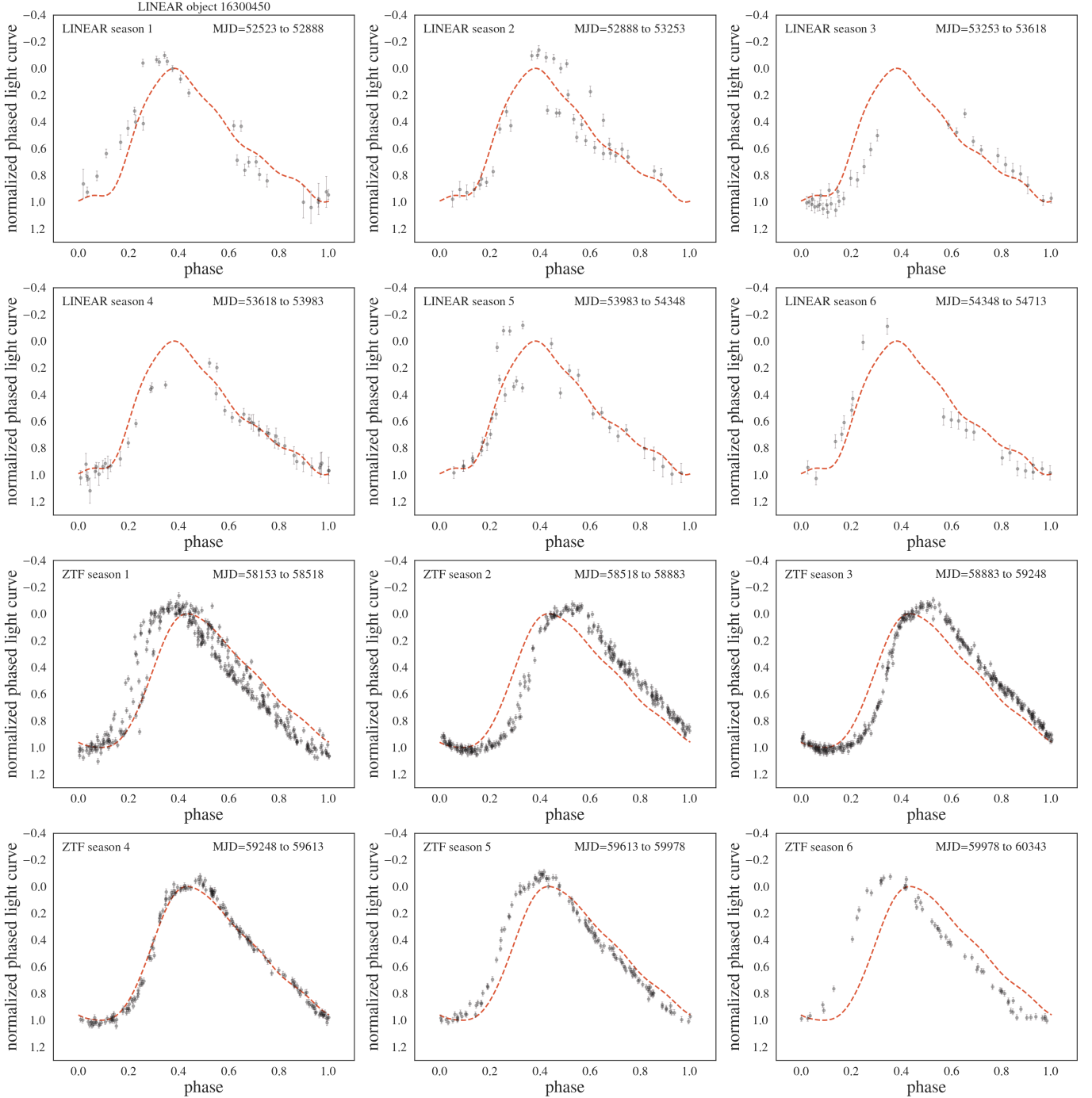


Figure 9. Analogous to Fig. 8, except that star with LINEARid = 16300450 is shown (period = 0.33562 day). Unlike example shown in Fig. 8, only phase modulation is visible here, without any amplitude modulation, in both LINEAR and ZTF light curves.

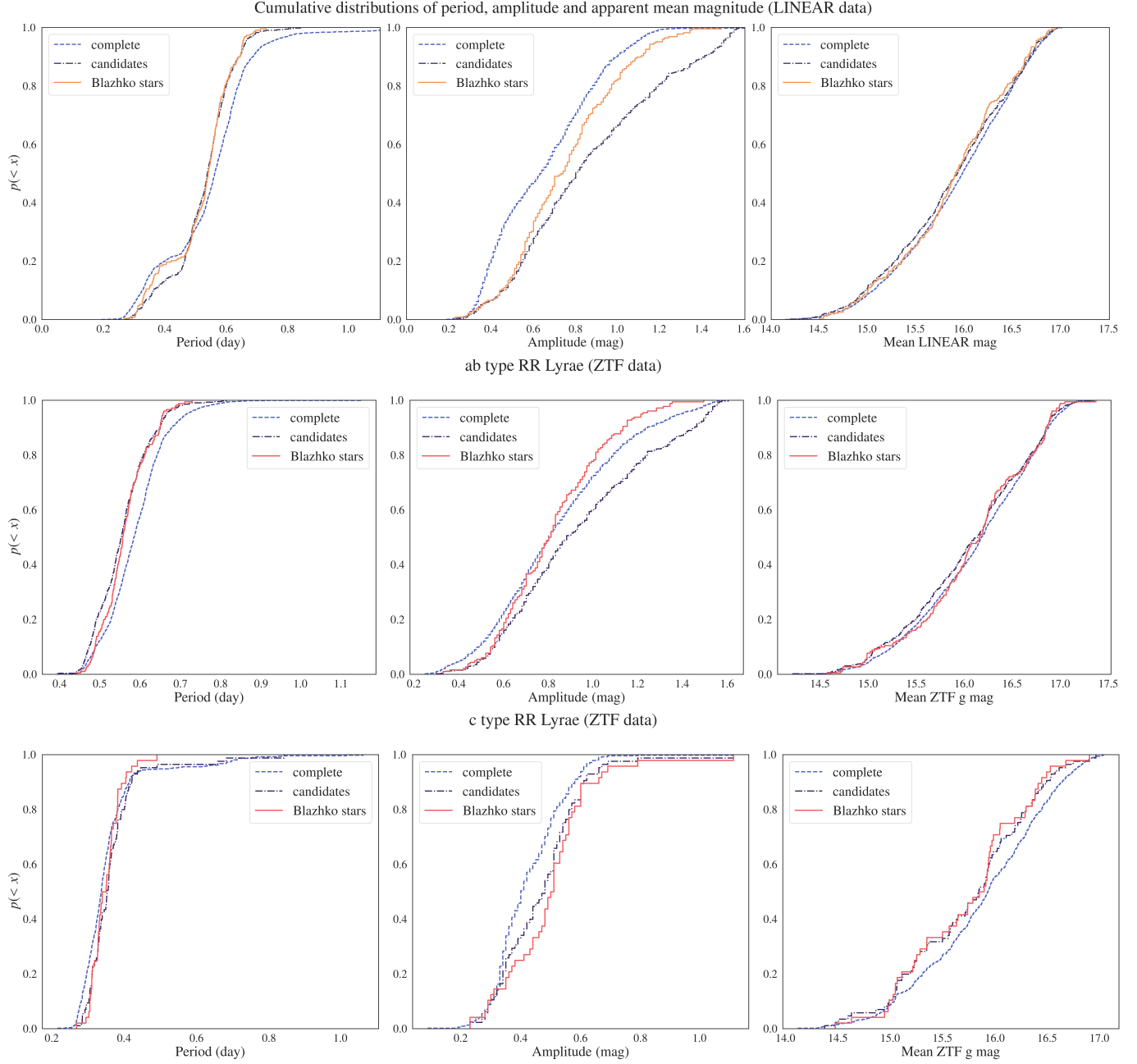


Figure 10. A comparison of cumulative distributions of period (left), amplitude (middle) and apparent magnitude for starting sample, selected Blazhko candidates and visually verified Blazhko stars. The top row is based on LINEAR data and both ab type and c type stars. The middle and bottom rows are based on ZTF data, and show separately data for ab type and c type stars, respectively. The differences in period and amplitude distributions are further examined in figure 11.

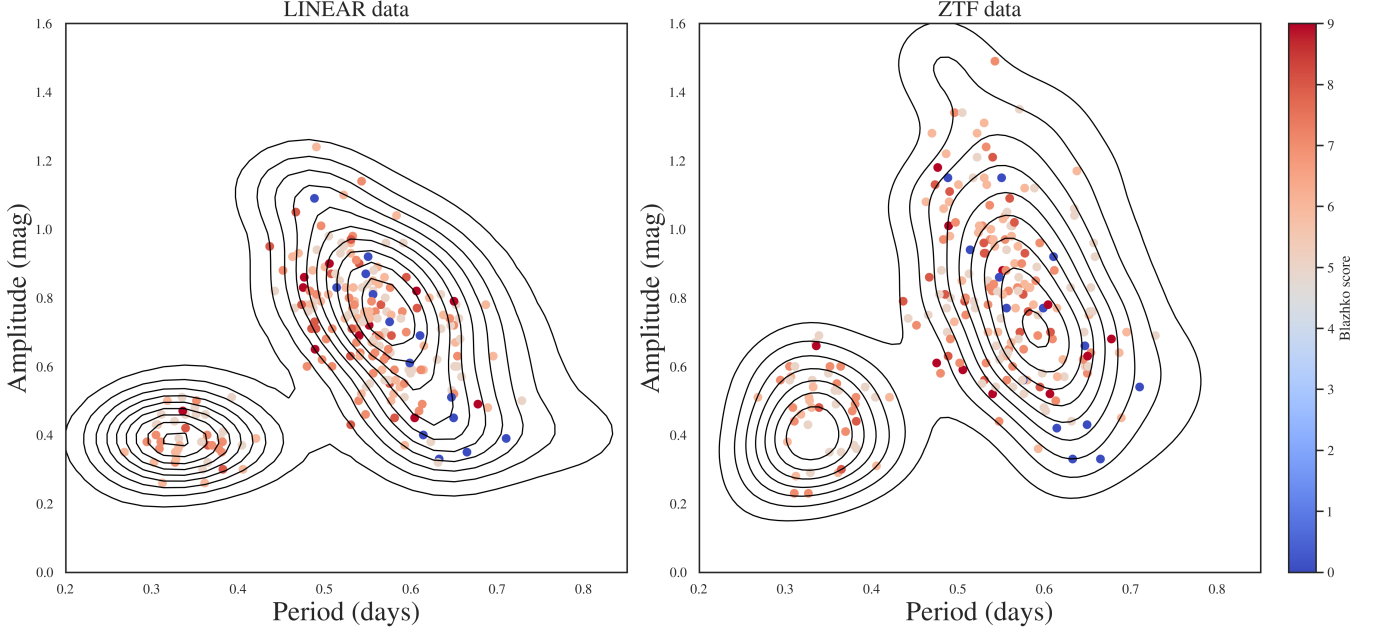


Figure 11. Comparison of amplitude–period distributions (the Bailey diagram) for the starting sample of 1,996 RR Lyrae stars (contours) and 228 selected candidate Blazhko stars (symbols). The clump in the lower left corresponds to c type RR Lyrae and the other one to ab type. Note that the period distribution for ab type Blazhko stars is shifted left (by about 0.03 day, or 5%).

530

LID	P _L	P _Z	N _L	N _Z	χ _{L,r} ²	χ _{Z,r} ²	χ _L ²	χ _Z ²	A _L	A _Z	δA	Bp _L	Bp _Z	Bp _L	Bp _Z	t	f	B _s	B _f
158779	0.609207	0.609189	293	616	1.6	3.9	3.7	34.2	0.47	0.68	0.21	1.6443	1.6444	352.7337	350.2	1	-	7	1
263541	0.558218	0.558221	270	503	2.9	6.6	15.8	110.4	0.64	0.82	0.18	1.8621	1.8025	14.1513	89.9	1	-	7	1
393084	0.530027	0.530033	493	372	1.1	3.2	1.6	19.2	0.96	1.31	0.35	1.9447	1.8896	17.2369	347.2	1	-	6	1
810169	0.465185	0.465212	289	743	2.1	2.8	6.0	15.1	0.77	0.75	0.02	2.2232	2.2230	13.6017	13.6	1	-	5	1
924301	0.507503	0.507440	418	189	1.9	9.3	13.8	162.9	0.87	0.79	0.08	2.0043	1.9763	29.5072	178.4	1	-	8	1
970326	0.592233	0.592231	275	552	1.1	2.1	1.9	7.7	0.51	0.75	0.24	1.7563	1.6992	14.7656	93.2	1	-	5	1
999528	0.658401	0.658407	564	213	1.2	2.7	1.8	21.7	0.57	0.92	0.35	1.5527	1.5510	29.5247	31.0	1	-	5	1
1005497	0.653607	0.653605	607	192	1.1	2.1	2.1	12.4	0.60	0.83	0.23	1.5639	1.5481	29.4638	55.1	1	-	5	1
1092244	0.649496	0.649558	590	326	1.2	3.6	2.3	32.1	0.72	0.58	0.14	1.5735	1.5640	29.5421	40.8	1	-	7	1
1240665	0.632528	0.632522	468	311	3.0	1.1	25.2	1.6	0.33	0.33	0.00	1.6149	1.5865	29.4942	182.3	1	Z	0	2

531

REFERENCES

- 532 Alcock, C., Alves, D. R., Becker, A., et al. 2003, ApJ, 598, 597, doi: [10.1086/378689](https://doi.org/10.1086/378689)
- 533 Astropy Collaboration, Price-Whelan, A. M., Sipőcz, B. M., et al. 2018, AJ, 156, 123, doi: [10.3847/1538-3881/aabc4f](https://doi.org/10.3847/1538-3881/aabc4f)
- 534 Astropy Collaboration, Price-Whelan, A. M., Lim, P. L., et al. 2022, ApJ, 935, 167, doi: [10.3847/1538-4357/ac7c74](https://doi.org/10.3847/1538-4357/ac7c74)
- 535 Bellm, E. C., Kulkarni, S. R., Graham, M. J., et al. 2019, PASP, 131, 018002, doi: [10.1088/1538-3873/aaecbe](https://doi.org/10.1088/1538-3873/aaecbe)
- 536 Benkő, J. M., Plachy, E., Szabó, R., Molnár, L., & Kolláth, Z. 2014, ApJS, 213, 31, doi: [10.1088/0067-0049/213/2/31](https://doi.org/10.1088/0067-0049/213/2/31)
- 537 Benkő, J. M., Szabó, R., & Paparó, M. 2011, MNRAS, 417, 974, doi: [10.1111/j.1365-2966.2011.19313.x](https://doi.org/10.1111/j.1365-2966.2011.19313.x)
- 538 Benkő, J. M., Kolenberg, K., Szabó, R., et al. 2010, MNRAS, 409, 1585, doi: [10.1111/j.1365-2966.2010.17401.x](https://doi.org/10.1111/j.1365-2966.2010.17401.x)
- 539 Blažko, S. 1907, Astronomische Nachrichten, 175, 325, doi: [10.1002/asna.19071752002](https://doi.org/10.1002/asna.19071752002)
- 540 Catelan, M. 2009, Ap&SS, 320, 261, doi: [10.1007/s10509-009-9987-8](https://doi.org/10.1007/s10509-009-9987-8)
- 541 Clementini, G., Ripepi, V., Garofalo, A., et al. 2023, A&A, 674, A18, doi: [10.1051/0004-6361/202243964](https://doi.org/10.1051/0004-6361/202243964)
- 542 Dagne, T. M., Berdnikov, L. N., Kniazev, A. Y., & Dambis, A. K. 2017, Information Bulletin on Variable Stars, 6228, 1, doi: [10.22444/IBVS.6228](https://doi.org/10.22444/IBVS.6228)

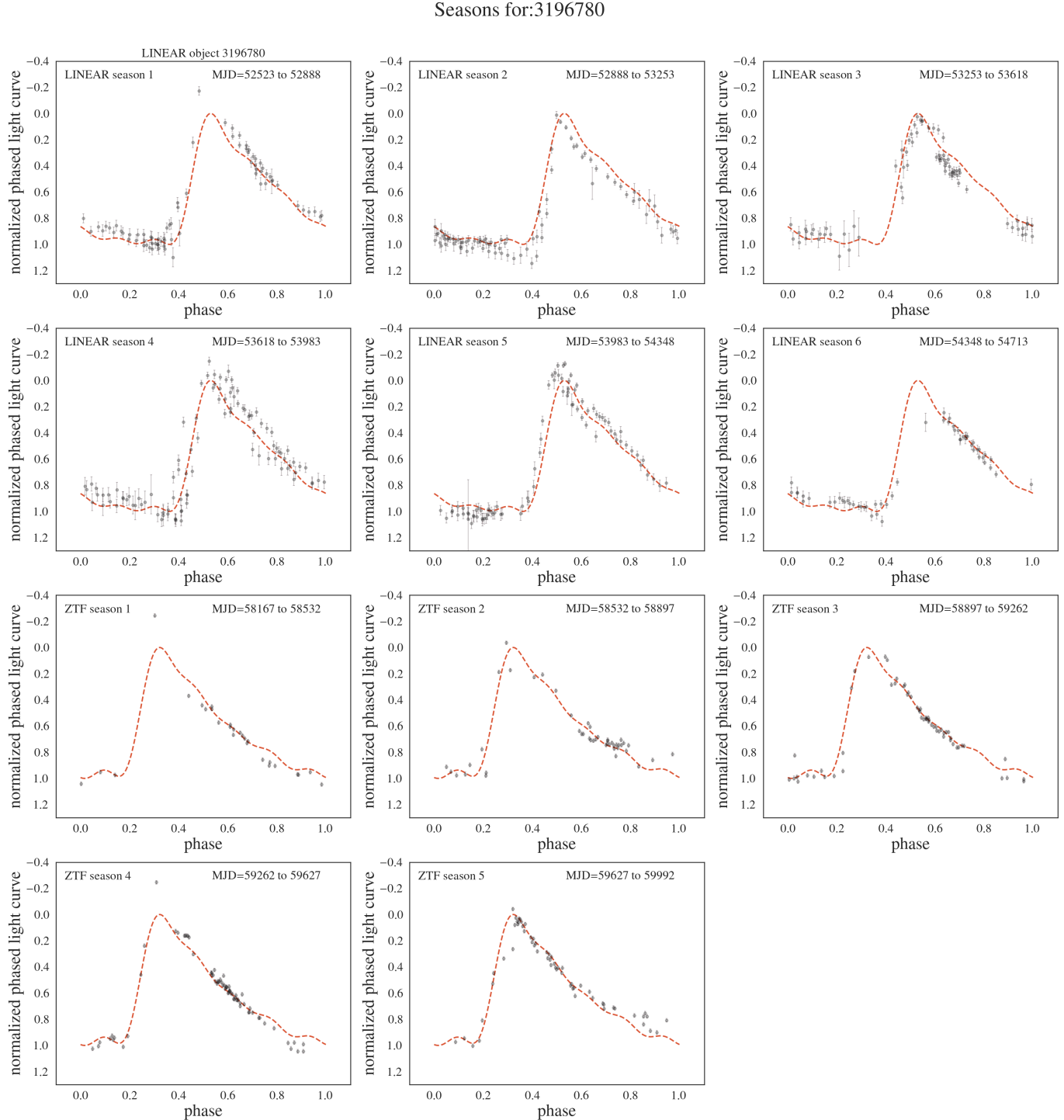


Figure 12. Analogous to Fig. 8, except that star with LINEARid = 3196780 is shown. Amplitude modulation is clearly seen in LINEAR light curves (top two rows), while not discernible in ZTF light curves (bottom two rows). Additional stars with similar behavior include LINEARid = 2889542, 7723614, 8342007. This behavior strongly suggests that Blazhko effect can appear and disappear on time scales shorter than about a decade.

- 556 Derekas, A., Kiss, L. L., Udalski, A., Bedding, T. R., &
 557 Szatmáry, K. 2004, MNRAS, 354, 821,
 558 doi: [10.1111/j.1365-2966.2004.08242.x](https://doi.org/10.1111/j.1365-2966.2004.08242.x)
- 559 Guggenberger, E., Kolenberg, K., Nemec, J. M., et al. 2012,
 560 MNRAS, 424, 649, doi: [10.1111/j.1365-2966.2012.21244.x](https://doi.org/10.1111/j.1365-2966.2012.21244.x)
- 561 Hajdu, G., Pietrzyński, G., Jurcsik, J., et al. 2021, ApJ,
 562 915, 50, doi: [10.3847/1538-4357/abff4b](https://doi.org/10.3847/1538-4357/abff4b)
- 563 Hernitschek, N., & Stassun, K. G. 2022, ApJS, 258, 4,
 564 doi: [10.3847/1538-4365/ac3baf](https://doi.org/10.3847/1538-4365/ac3baf)
- 565 Hunter, J. D. 2007, Computing in Science & Engineering, 9,
 566 90, doi: [10.1109/MCSE.2007.55](https://doi.org/10.1109/MCSE.2007.55)
- 567 Ivezić, Ž., Kahn, S. M., Tyson, J. A., et al. 2019, ApJ, 873,
 568 111, doi: [10.3847/1538-4357/ab042c](https://doi.org/10.3847/1538-4357/ab042c)
- 569 Jurcsik, J., Sóder, Á., Szeidl, B., et al. 2009, MNRAS, 400,
 570 1006, doi: [10.1111/j.1365-2966.2009.15515.x](https://doi.org/10.1111/j.1365-2966.2009.15515.x)
- 571 Kolenberg, K. 2008, in Journal of Physics Conference
 572 Series, Vol. 118, Journal of Physics Conference Series
 573 (IOP), 012060, doi: [10.1088/1742-6596/118/1/012060](https://doi.org/10.1088/1742-6596/118/1/012060)
- 574 Kovács, G. 2009, in American Institute of Physics
 575 Conference Series, Vol. 1170, Stellar Pulsation:
 576 Challenges for Theory and Observation, ed. J. A. Guzik
 577 & P. A. Bradley, 261–272, doi: [10.1063/1.3246458](https://doi.org/10.1063/1.3246458)
- 578 Kovacs, G. 2016, Communications of the Konkoly
 579 Observatory Hungary, 105, 61,
 580 doi: [10.48550/arXiv.1512.05722](https://doi.org/10.48550/arXiv.1512.05722)
- 581 —. 2018, A&A, 614, L4, doi: [10.1051/0004-6361/201833181](https://doi.org/10.1051/0004-6361/201833181)
- 582 Le Borgne, J. F., & Klotz, A. 2019, arXiv e-prints,
 583 arXiv:1902.00905, doi: [10.48550/arXiv.1902.00905](https://doi.org/10.48550/arXiv.1902.00905)
- 584 Mizerski, T. 2003, AcA, 53, 307,
 585 doi: [10.48550/arXiv.astro-ph/0401612](https://doi.org/10.48550/arXiv.astro-ph/0401612)
- 586 Molnár, L., Plachy, E., Bódi, A., et al. 2023, A&A, 678,
 587 A104, doi: [10.1051/0004-6361/202346507](https://doi.org/10.1051/0004-6361/202346507)
- 588 Netzel, H., Smolec, R., Soszyński, I., & Udalski, A. 2018,
 589 MNRAS, 480, 1229, doi: [10.1093/mnras/sty1883](https://doi.org/10.1093/mnras/sty1883)
- 590 Palaversa, L., Ivezić, Ž., Eyer, L., et al. 2013, AJ, 146, 101,
 591 doi: [10.1088/0004-6256/146/4/101](https://doi.org/10.1088/0004-6256/146/4/101)
- 592 Poretti, E., Paparó, M., Deleuil, M., et al. 2010, A&A, 520,
 593 A108, doi: [10.1051/0004-6361/201014941](https://doi.org/10.1051/0004-6361/201014941)
- 594 Prudil, Z., & Skarka, M. 2017, MNRAS, 466, 2602,
 595 doi: [10.1093/mnras/stw3231](https://doi.org/10.1093/mnras/stw3231)
- 596 Sesar, B., Stuart, J. S., Ivezić, Ž., et al. 2011, AJ, 142, 190,
 597 doi: [10.1088/0004-6256/142/6/190](https://doi.org/10.1088/0004-6256/142/6/190)
- 598 Sesar, B., Ivezić, Ž., Grammer, S. H., et al. 2010, ApJ, 708,
 599 717, doi: [10.1088/0004-637X/708/1/717](https://doi.org/10.1088/0004-637X/708/1/717)
- 600 Sesar, B., Ivezić, Ž., Stuart, J. S., et al. 2013, AJ, 146, 21,
 601 doi: [10.1088/0004-6256/146/2/21](https://doi.org/10.1088/0004-6256/146/2/21)
- 602 Skarka, M. 2013, A&A, 549, A101,
 603 doi: [10.1051/0004-6361/201220398](https://doi.org/10.1051/0004-6361/201220398)
- 604 Skarka, M., Prudil, Z., & Jurcsik, J. 2020, MNRAS, 494,
 605 1237, doi: [10.1093/mnras/staa673](https://doi.org/10.1093/mnras/staa673)
- 606 Smith, H. A. 1995, Cambridge Astrophysics Series, 27
- 607 Sóder, Á., Skarka, M., Liška, J., & Bognár, Z. 2017,
 608 MNRAS, 465, L1, doi: [10.1093/mnrasl/slw194](https://doi.org/10.1093/mnrasl/slw194)
- 609 Soszyński, I., Udalski, A., Szymański, M. K., et al. 2010,
 610 AcA, 60, 165, doi: [10.48550/arXiv.1009.0528](https://doi.org/10.48550/arXiv.1009.0528)
- 611 —. 2009, AcA, 59, 1, doi: [10.48550/arXiv.0903.2482](https://doi.org/10.48550/arXiv.0903.2482)
- 612 Soszyński, I., Dziembowski, W. A., Udalski, A., et al. 2011,
 613 AcA, 61, 1, doi: [10.48550/arXiv.1105.6126](https://doi.org/10.48550/arXiv.1105.6126)
- 614 Szabó, R. 2014, in IAU Symposium, Vol. 301, Precision
 615 Asteroseismology, ed. J. A. Guzik, W. J. Chaplin,
 616 G. Handler, & A. Pigulski, 241–248,
 617 doi: [10.1017/S1743921313014397](https://doi.org/10.1017/S1743921313014397)
- 618 Szabó, R., Benkő, J. M., Paparó, M., et al. 2014, A&A,
 619 570, A100, doi: [10.1051/0004-6361/201424522](https://doi.org/10.1051/0004-6361/201424522)
- 620 Szczygieł, D. M., & Fabrycky, D. C. 2007, MNRAS, 377,
 621 1263, doi: [10.1111/j.1365-2966.2007.11678.x](https://doi.org/10.1111/j.1365-2966.2007.11678.x)
- 622 Szeidl, B., Hurta, Z., Jurcsik, J., Clement, C., & Lovas, M.
 623 2011, MNRAS, 411, 1744,
 624 doi: [10.1111/j.1365-2966.2010.17815.x](https://doi.org/10.1111/j.1365-2966.2010.17815.x)
- 625 Vanderplas, J. 2015, gatspy: General tools for Astronomical
 626 Time Series in Python, v0.1.1, Zenodo,
 627 doi: [10.5281/zenodo.14833](https://doi.org/10.5281/zenodo.14833)
- 628 VanderPlas, J., Connolly, A. J., Ivezić, Z., & Gray, A.
 629 2012, in Proceedings of Conference on Intelligent Data
 630 Understanding (CIDU, 47–54,
 631 doi: [10.1109/CIDU.2012.6382200](https://doi.org/10.1109/CIDU.2012.6382200)
- 632 Virtanen, P., Gommers, R., Oliphant, T. E., et al. 2020,
 633 Nature Methods, 17, 261, doi: [10.1038/s41592-019-0686-2](https://doi.org/10.1038/s41592-019-0686-2)